

ARTICLE

Open Access



Osthole ameliorates myonecrosis caused by *Clostridium perfringens* type A infection in mice

Xueyong Zhang^{1,2†}, Yue Liu^{1,2†}, Zhangqi Shen^{1,2}, Shaolin Wang^{1,2}, Congming Wu^{1,2}, Dejun Liu^{1,2}, Shusheng Tang^{1,2} and Chongshan Dai^{1*}

Abstract

This study aimed to investigate the protective effect of the nature product osthole (OST) against *Clostridium perfringens* type A infection-caused myonecrosis in a mouse model. Male mice were divided into (1) control, (2) infected, (3) OST50 and (4) OST100 treatment groups. In the infected groups, mice were intramuscularly injected with 1×10^8 CFU of *C. perfringens* per day for 6 days. Mice in the OST50 and OST100 groups were administrated intraperitoneally with OST at the doses of 50 or 100 mg/kg per day post *C. perfringens* infection. Our results showed that *C. perfringens* infection caused marked necrosis and inflammatory cell infiltration in the muscle tissues of mice. Mice in the OST50 and OST100 treatment groups displayed significantly attenuated *C. perfringens* infection-induced lipid peroxidation, oxidative stress, and apoptosis in their muscle tissue. Furthermore, OST treatment significantly downregulated the expressions of NF- κ B, IL-1 β , and TNF- α mRNA and protein levels, while concomitantly upregulating the expressions of Nrf2 and HO-1 mRNA and protein. OST treatments also inhibited the expression of phosphorylation (p)-p38, p-mTOR, and p-Erk1/2 proteins, and upregulated LC3II and Beclin1 proteins. In summary, our results reveal that OST therapy confers a protective effect against *C. perfringens* infection-induced oxidative stress and inflammation in muscle tissue, via activation of Nrf2/HO-1 and autophagy pathways and inhibition of p38, Erk1/2 and NF- κ B pathways.

Keywords *C. perfringens*, Myonecrosis, Osthole, Nrf2/HO-1 pathway, NF- κ B pathway

Introduction

Clostridium (C.) perfringens type A is a spore-forming Gram-positive, anaerobic bacterium that causes gas gangrene, sepsis, necrotic enteritis, and diarrhea in humans and livestock [1]. *C. perfringens* type A is a global leading

cause of food poisoning [2], in the United States alone, it is responsible for about 14% of all food poisoning cases [2]. Notably, gas gangrene which is also called clostridial myonecrosis, can lead to loss of cardiac function disruption and even death [3, 4]. Furthermore, *C. perfringens* has developed resistance against several antibiotics, including minocycline, enrofloxacin, erythromycin, tetracycline, tylosin, florfenicol, and bacitracin [5, 6]. Therefore, urgent efforts are needed to develop novel therapeutic strategies to combat infections caused by multi-drug resistant *C. perfringens* type A.

C. perfringens type A produces alpha (α)-toxin, (*syn.* phospholipase C (PLC)), which is a critical pathogenic factor in humans and livestock during *C. perfringens* type A infection [4, 7]. *C. perfringens* α -toxin exposure

[†]Xueyong Zhang and Yue Liu contributed equally to this work.

*Correspondence:

Chongshan Dai
daichongshan@cau.edu.cn

¹ National Key Laboratory of Veterinary Public Health and Safety, College of Veterinary Medicine, China Agricultural University, Beijing 100193, China

² Guangdong Laboratory for Lingnan Modern Agriculture, Guangzhou 510642, China



induces the formation of platelet-leukocyte aggregates, leading to the impediment of neutrophil extravasation, ultimately resulting in immune dysfunction [8, 9]. Several key immuno-inflammatory and redox signaling pathways, including the reactive oxygen species (ROS)-mediated oxidative stress pathway, mitogen-activated protein kinase (MAPK)/extracellular signal-regulated kinase1/2 (Erk1/2) pathway, nuclear factor kappa-B (NF- κ B) pathway, toll-like receptor 4 (TLR4) pathway, NOD-like receptor family pyrin domain-containing 3 (NLRP3), TLR2 pathway, and p38 MAPK pathway, have been reported to be involved in the pathogenicity of *C. perfringens* type A infection in host cells [1, 3, 10, 11]. There have been numerous reports supporting the protective benefits of natural products such as piceatannol, amentoflavone, and verbascoside, that appear to ameliorate the (α)-toxin induced pathogenicity of *C. perfringens* type A infection [12–14].

Osthole (OST), a coumarin derivative extracted from *Cnidium monnieri*, exhibits a multitude of beneficial biological effects, including anti-inflammatory and antioxidant [15–20]. Notably, OST has been reported to activate nuclear factor erythroid 2-related factor 2 (Nrf2) expression, which plays a critical role in regulating oxidative stress and inflammatory response [21, 22].

OST also inhibits lipopolysaccharide-induced inflammatory responses and lung damage by inhibiting the nuclear translocation of NF- κ B [18]. OST supplementation has been reported to effectively inhibit *Staphylococcus aureus* infection-induced lung inflammation in mice by inhibiting the production of the virulence factor α -hemolysin [15]. Thus far, investigations of the potential therapeutic benefits of OST against *C. perfringens*-induced inflammation and myonecrosis have been limited. In the present study, we report the protective effects of OST supplementation against *C. perfringens* type A induced myonecrosis in the muscle tissues of mice. Importantly, for the first time, we reveal that the potential action mechanisms involve the stabilizing regulation of autophagy, MAPKs, Nrf2, and NF- κ B signaling pathways.

Results

OST supplementation ameliorates *C. perfringens* infection-caused histopathological changes in the muscle tissues of mice

As shown in Fig. 1A, *C. perfringens* infection caused marked muscle necrosis in gross anatomical level. The muscle tissues of infected mice in the OST50 and OST100 treatments groups displayed a significant

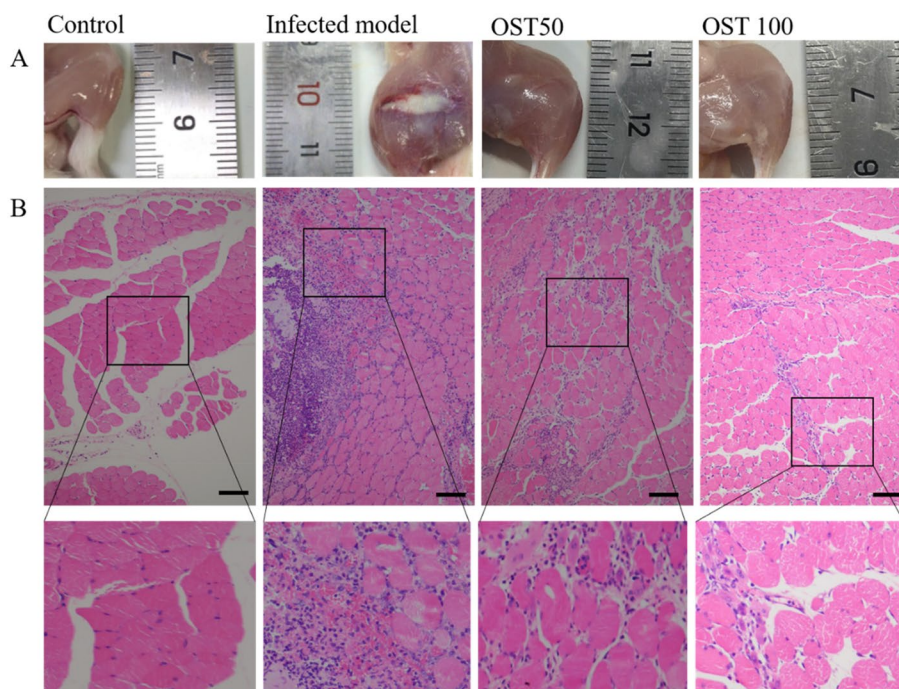


Fig. 1 The representative images of gross (A) and histopathological (B) examinations of muscle tissues. Mice in the untreated control group were treated with an equal volume of vehicle (i.e., 0.5% DMSO). In the infected model group, mice were intramuscularly injected with 1×10^8 CFU of *C. perfringens* C57-1 stain per day for 6 days. In the OST50 and OST100 treatment groups, mice were intramuscularly injected with *C. perfringens* C57-1 stain for 6 days with the co-treatments of OST at the doses of 50 and 100 mg/kg per day for 7 days. Bar = 100 μ m

improvement compared to the untreated group. Furthermore, H&E staining was performed to assess the histopathological changes. Mice in *C. perfringens* infection model group showed areas of myonecrosis, which was characterized by myofibrillar hypercontraction of myofiber and reduced numbers with massive inflammatory infiltrate (Fig. 1B). OST supplementation at 50 and 100 mg/kg/day for continuous 7 days significantly reduced the areas of myonecrosis and inflammatory cells infiltrate in the muscle tissues, compared to those in the infected model group (Fig. 1B).

OST supplementation reduces the bacterial burden of infected muscle tissue

Following seven days of treatment, the bacterial burden was assessed in the infected muscle tissues. As shown in the Fig. 2A, Gram-staining revealed Gram-positive bacilli in the peripheral areas of the infected muscle. The OST50 and OST100 groups all displayed reduced *C. perfringens* in the infected muscle. Furthermore, the bacterial enumeration in the infected muscle was counted using the agar plate method. As shown in Fig. 2B, OST treatment at doses of 50 and 100 mg/kg/day significantly reduced the bacterial CFU in the infected muscle, compared to that in the infected model group.

OST supplementation ameliorates *C. perfringens* infection-caused oxidative stress damage in the muscle tissues

Marked changes in biomarkers of oxidative stress were detected in the *C. perfringens* infected muscle tissues. Compared to the untreated control group, the muscle

tissues of the infected mice displayed increased levels of MDA (5.63 nmol/mg protein) and decreased activities of SOD (39.2 U/mg protein) and CAT (0.91 U/mg protein) (all $P < 0.001$) (Fig. 3). OST supplementation significantly improved the redox imbalance of muscle tissues caused by *C. perfringens* infection. In the OST 50 and OST100 treatment groups, the MDA levels significantly decreased to 3.69 nmol/mg protein and 2.90 nmol/mg protein (both $P < 0.001$), respectively (Fig. 3A). The activities of SOD significantly increased to 57.8 U/mg protein, and 63.4 U/mg protein (both $P < 0.001$), respectively (Fig. 3B), while the activities of CAT showed significant increments to 1.47 U/mg protein and 1.91 U/mg protein ($P < 0.01$ or $P < 0.001$), respectively (Fig. 3C).

OST supplementation downregulates the levels of caspases-9 and -3 activities in the muscle tissues of mice

As shown in Fig. 4, *C. perfringens* infection significantly increased the activities of caspases-9 and -3 in the muscle tissues of mice. Compared to the uninfected control group, *C. perfringens* infection increased the activities of caspases-9 and -3 to 3.87-fold and 3.17-fold (both $P < 0.001$), respectively. OST supplementation significantly inhibited the activation of caspases-9 and -3 in the infected muscle tissues. In the OST50 treatment group, the activities of caspases-9 and -3 were significantly decreased to 2.32-fold ($P < 0.001$), and 2.20-fold ($P < 0.01$), respectively. Meanwhile, in the OST100 treatment group, the activities of caspases-9 and -3 significantly decreased to 1.58-fold, and 1.67-fold (both $P < 0.001$), respectively.

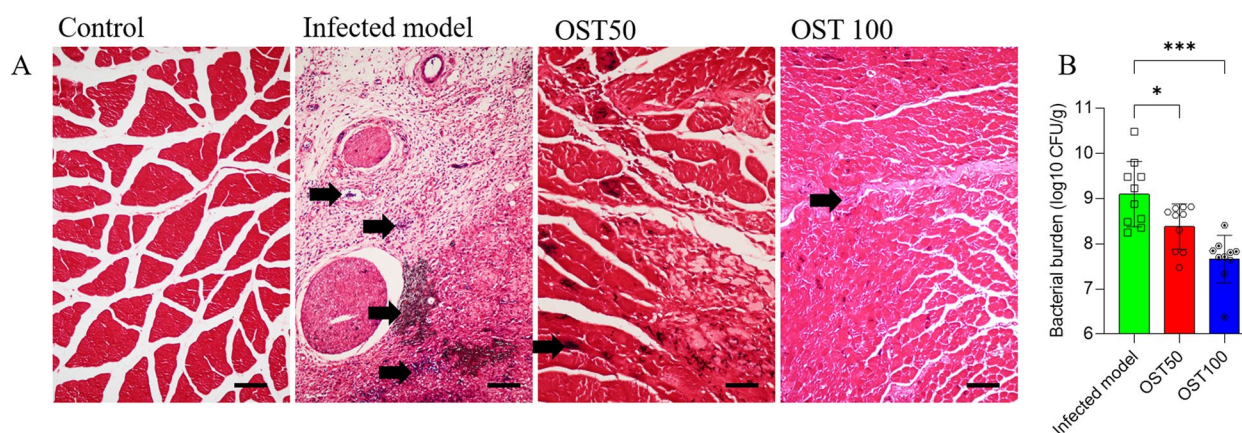


Fig. 2 Bacterial burden in the muscle tissues of mice infected with *C. perfringens* both with and without OST supplementation. **A** The representative images of Gram-staining. **B** The bacterial enumeration was counted in the infected muscles. Bar = 100 μ m. Data were expressed as mean \pm S.D ($n = 10$). * $P < 0.05$ and *** $P < 0.001$, compared between the two groups. Black arrows indicate the Gram-positive bacteria

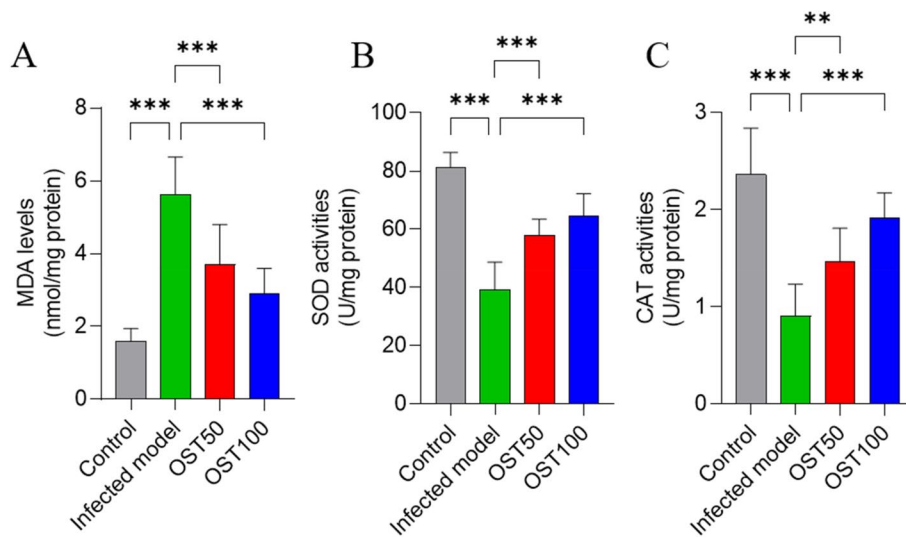


Fig. 3 Biomarkers of oxidative stress in the muscle tissues of mice infected with *C. perfringens* both with and without OST supplementation. **A** The levels of MDA. **B** The activities of SOD. **C**, the activities of CAT. All data were presented as mean ± S.D. (n = 10). **P < 0.01 and ***P < 0.001, compared between the two groups

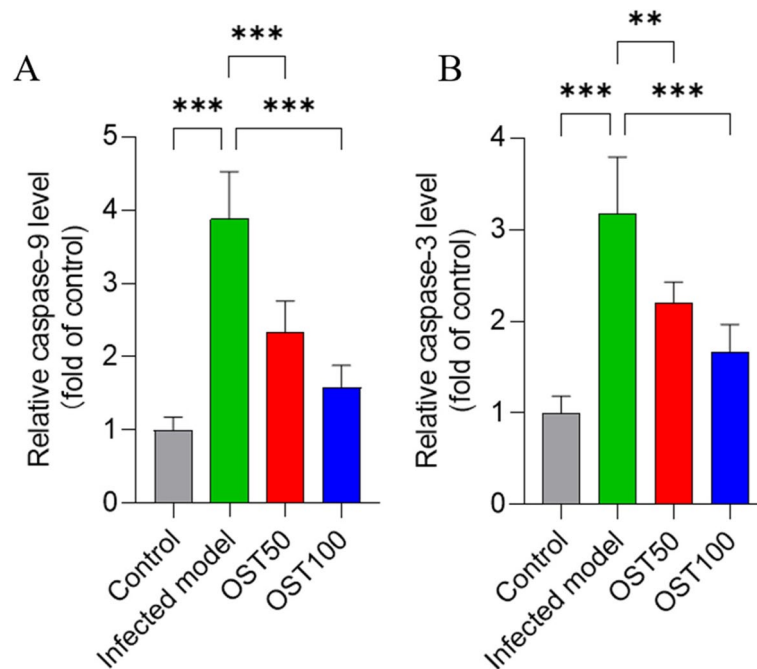


Fig. 4 The levels of caspases-9 and -3 activities in the muscle tissues of mice. **A** The caspase-9 activities. **B** The caspase-3 activities. All data were presented as mean ± S.D. (n = 6). **P < 0.01, and ***P < 0.001, compared between the two groups

OST supplementation reduces *C. perfringens* infection-caused inflammatory response in the muscle tissues of mice

Compared to the uninfected control group, *C. perfringens* infection significantly increased the levels of IL-1β and TNF-α proteins to 64.2 pg/mg protein and 39.0 pg/mg

protein (both P < 0.001) (Fig. 5), respectively. In contrast, in the OST50 treatment group, the levels of IL-1β and TNF-α proteins were significantly decreased to 50.2 pg/mg protein and 30.6 pg/mg protein (both P < 0.05), respectively. Similarly, in the OST100 treatment group, the levels of IL-1β and TNF-α proteins significantly

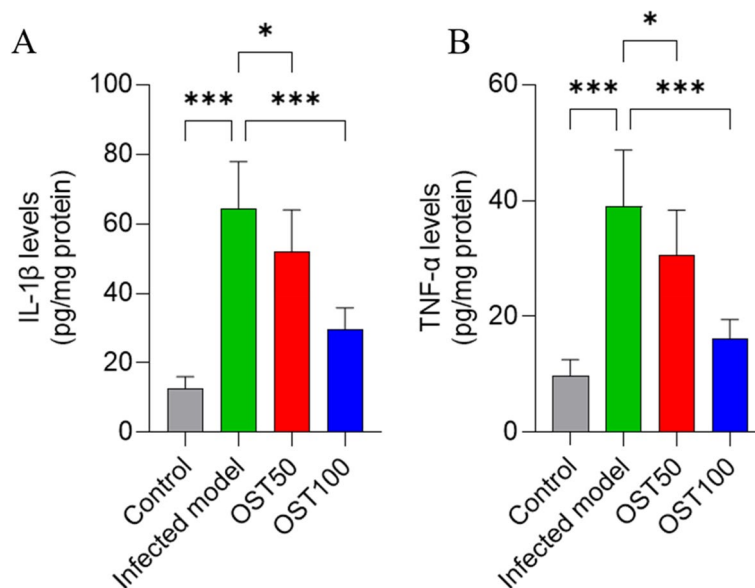


Fig. 5 The levels of IL-1 β (A) and TNF- α (B) in the muscle tissue of mice. All data were presented as mean \pm S.D. ($n=6$). * $P<0.05$, and *** $P<0.001$, compared between the two groups

decreased to 29.7 pg/mg protein and 16.2 pg/mg protein (both $P<0.001$), respectively.

OST supplementation upregulates the expressions of Nrf2, HO-1, Beclin1, and LC3II proteins, and downregulates the expressions of p-p38, p-Erk1/2, NF- κ B, p-mTOR proteins in the muscle tissues of mice

Compared to the uninfected control group, *C. perfringens* infection significantly upregulated the expressions of p-p38, p-JNK1/2, p-Erk1/2, Nrf2, HO-1, p-mTOR, LC3II, and NF- κ B proteins to 5.31-, 2.51-, 11.5-, 2.02-, 3.25-, 4.10-, 1.87-, and 1.98-fold, respectively (all $P<0.05$, 0.01 or 0.0001), and significantly downregulated the expression of Beclin1 protein to 0.55-fold ($P<0.01$) (Fig. 6). OST supplementation could regulate the expressions of these proteins. Especially, in the OST100 treatment group, the expressions of Nrf2, HO-1, Beclin1, and LC3II proteins were upregulated to 4.48-, 10.4-, 2.05-, and 4.19- fold (all $P<0.0001$), respectively, and significantly downregulated the expression of p-p38, p-Erk, p-mTOR, and NF- κ B proteins to 2.23-, 3.11-, 1.32-, and 0.54-fold (all $P<0.0001$), respectively (Fig. 6). However, OST treatments did not change the expression of p-JNK1/2 protein, compared to that in the infected model group (Fig. 6).

OST supplementation regulates the expression of genes enriched in Nrf2/HO-1 and NF- κ B pathways

Compared to the uninfected control group, *C. perfringens* infection significantly upregulated the expressions of NF- κ B, TNF- α , IL-1 β , Nrf2, and HO-1

mRNAs to 5.67-, 11.1-, 6.17-, 1.95-, and 2.77-fold (all $P<0.05$, or 0.0001) (Suppl. Figure 2), respectively. OST supplementation at the doses of 50 or 100 mg/kg/day for 7 days could effectively regulate the expression of these genes. Especially, in the OST100 treatment group, the expressions of NF- κ B, TNF- α , and IL-1 β mRNAs were significantly downregulated to 1.98-, 3.49-, and 2.10-fold (all $P<0.001$) (Suppl. Figure 2), respectively, whereas the expression of Nrf2 and HO-1 mRNAs were further upregulated to 3.39- and 5.08-fold (both $P<0.001$) (Suppl. Figure 2), respectively. * $P<0.05$, ** $P<0.01$, and *** $P<0.001$, compared between the two groups.

Discussion

C. perfringens is a Gram-positive, anaerobic, spore-forming, and rod-shaped pathogen [23]. It is known to produce an arsenal of >20 virulent toxins [23], including α -toxin, β -toxin, epsilon-toxin, iota-toxin, enterotoxin, and necrotic enteritis B-like toxin [24]. *C. perfringens* type A commonly causes life-threatening infections, including gas gangrene, septicemia, and necrotic enteritis [24].

In the present study, we provide demonstrable evidence of the protective benefits of OST supplementation via intraperitoneal injection at the doses of 50 mg/kg/day (cumulative dose 350 mg/kg) and 100 mg/kg/day (cumulative dose 700 mg/kg) for 7 days, which could both effectively improve *C. perfringens* C57-1 induced myonecrosis and reduced the bacterial burden (Figs. 1 and 2). Furthermore, our results showed

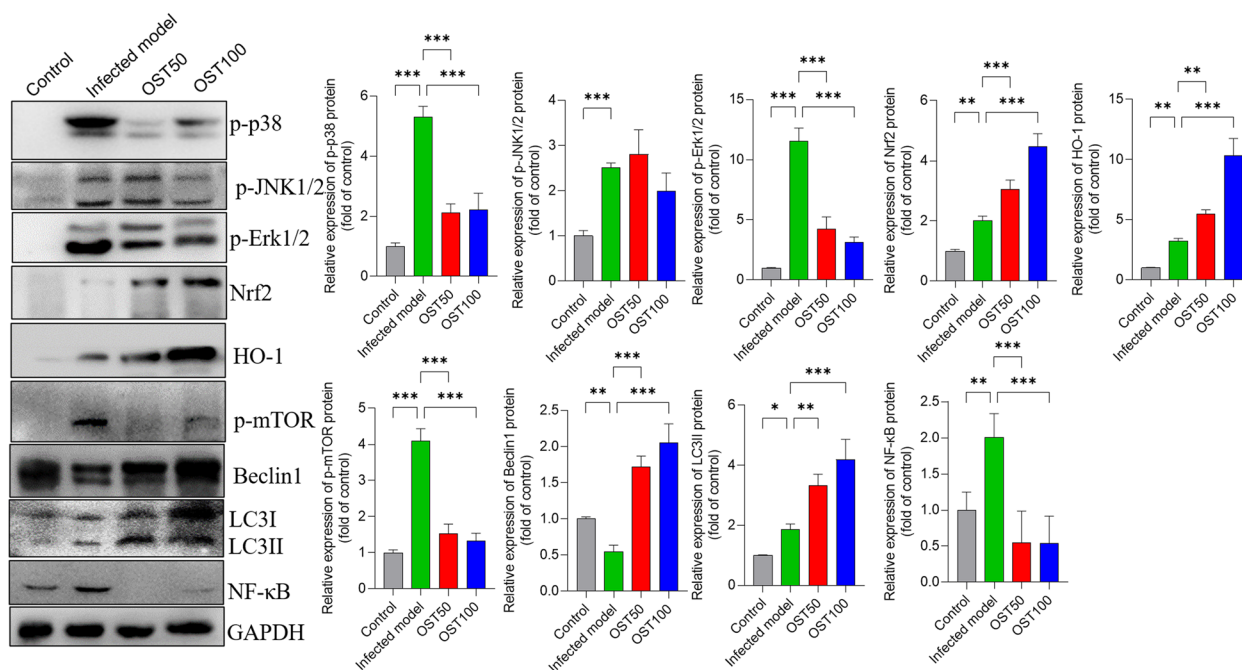


Fig. 6 Effects of OST supplementation on the protein expressions in the muscle tissues of mice. The expressions of p-p38, p-JNK1/2, p-Erk1/2, Nrf2, HO-1, p-mTOR, Beclin1, LC3II, and NF-κB proteins in the muscle tissues of mice were analyzed using Western Blotting. The representative images were presented (on the left) and the values of each band were analyzed quantitatively using Image J software (on the right). All results were presented as mean \pm SD ($n=4$). ** $P < 0.01$, and *** $P < 0.001$, compared between the two groups

that OST supplementation could effectively attenuate *C. perfringens* C57-1 induced oxidative stress and immunoinflammatory responses via stabilizing regulation of the Nrf2/HO-1, MAPK, NF-κB and autophagy pathways (Figs. 2, 3, 4, 5, 6 and Suppl. Figure 2).

Previous studies have demonstrated that α -toxin is the major virulence factor of *C. perfringens* A type involved in gas gangrene pathogenesis [25, 26]. Monturiol-Gross *et al.*, reported that *C. perfringens* α -toxin exposure at the lower dose (i.e., 4 ng/mL) significantly induced excessive production of reactive oxygen species (ROS), which could be markedly inhibited by various antioxidants such as glutathione monomethyl ester, *N*-acetyl-L-cysteine, CAT, and tiron [3]. In the present study, we found that *C. perfringens* C57-1 infection significantly upregulated the levels of MDA, and significantly downregulated the activities of antioxidant enzymes SOD and CAT (Fig. 3). These findings suggest that oxidative stress plays an important role in *C. perfringens* A pathogenesis. OST supplementation reversed these effects and significantly decreased the levels of MDA, and upregulated the activities of SOD and CAT (Fig. 3). Similarly, Zhou *et al.*, reported that OST supplementation at a dose of 100 mg/kg via intraperitoneal injection markedly attenuated tamoxifen-induced oxidative stress injury in the liver tissue of mice [27]. Taken together, these data indicated

that OST supplementation could offer a protective effect against myonecrosis caused by *C. perfringens* A type infection via the inhibition of lipid peroxidation and the upregulation of antioxidant enzymes activities.

It is well known that *C. perfringens* α -toxin could also directly disrupt cell membranes of mammalian cells, rapidly resulting in cytolysis/hemolysis [28]. Moreover, *C. perfringens* α -toxin is known to induce cell apoptosis via mitochondrial damage in the isolated skeletal muscle [29]. Manni *et al.*, found that *C. perfringens* α -toxin treatment of GM95 cells elevated the release of cytochrome C from mitochondria, caspases-9 and -3 activation [30]. Similarly, our results showed that *C. perfringens* A type infection markedly increased caspases-9 and -3 activities in the muscle tissues of mice, and these apoptosis markers were partly abolished in the OST supplementation groups (Fig. 4). In a previous study, Xia *et al.*, found that intraperitoneal administration of OST at the doses of 10–30 mg/kg for 14 days protected against cortical stab wound injury-induced neuronal apoptosis in mice [31]. Taken together, these data indicated that OST supplementation could attenuate *C. perfringens* induced apoptosis in the muscle tissues of mice, which may partly be attributed to the inhibition of the mitochondrial apoptosis pathway. Moreover,

mitochondria are a critical target of ROS [32]. Many studies have demonstrated that the inhibition of ROS production could effectively ameliorate mitochondrial dysfunction and block the activation of the mitochondrial apoptotic pathway [3, 32, 33]. Therefore, the ameliorative effects conferred by OST supplementation in the muscle tissues of mice may be partly associated with its inhibition of ROS production.

The immuno-inflammatory response is one of the main events associated with *C. perfringens* type A induced myonecrosis in humans and animals [11, 34, 35]. Guo *et al.*, reported that *C. perfringens* α -toxin exposure of primary chicken intestinal epithelial cells activated the expression of NF- κ B and its downstream proinflammatory factors, including TNF- α , IL-6, IL-8, and inducible nitric oxide synthase (iNOS) [10]. Similarly, in the present study, *C. perfringens* infection significantly upregulated the expression of NF- κ B, IL-1 β , and TNF- α mRNA and protein levels in the muscle tissue of mice (Figs. 5 and 6; Suppl. Figure 2); these untoward effects were reversed in response to OST treatment (Figs. 5 and 6; Suppl. Figure 2). Notably, previous studies have showed that NF- κ B is a critical target in the OST-mediated anti-inflammatory response [20, 36, 37].

C. perfringens α -toxin has been demonstrated to directly interact with tyrosine kinase A, consequently activating the Erk1/2 and p38 signaling pathways [38]. Consistently, Monturiol-Gross *et al.*, reported that the activation of NF- κ B by *C. perfringens* α -toxin exposure is mainly dependent on the expression of Erk1/2 [39]. In the present study, our results showed that *C. perfringens* infection significantly upregulated the expression of p-Erk1/2, p38, and p-JNK1/2 protein levels (Fig. 6). OST supplementation significantly abolished the expression of p-Erk1/2 and p38 proteins; however, it did not impact the expression of p-JNK1/2 (Fig. 6).

Several studies have demonstrated OST as an inducer of Nrf2, a critical transcription factor in regulating oxidative stress and the inflammatory response [20]. For example, Tang *et al.*, reported that OST supplementation at a dose of 25 mg/kg/day for 14 days significantly upregulated the expression of Nrf2 and HO-1 proteins in the brain, protecting against chronic sleep deprivation-induced memory impairment in rats [40]. García-Arroyo *et al.*, showed that oral supplementation with OST at a dose of 40 mg/kg/day for 30 days significantly upregulated the expression of Nrf2, HO-1, CAT, and SOD proteins in the kidneys of rats, which conferred a protective role against high-fat/high-sugar diet-induced chronic renal damage [41]. Consistently, our current study found that OST supplementation significantly upregulated the expressions of Nrf2 and HO-1 mRNA and protein levels, and elevated the levels of CAT and

SOD in the muscle tissues of infected mice (Figs. 3 and 6; Suppl. Figure 2).

LC3-II and Beclin1 are key biomarkers of autophagic flux, as they respectively mediate the initiation and closure of the autophagic vesicle [42, 43]. Conway *et al.*, showed that activation of the autophagy related gene 16L1 (ATG16L1)-mediated the clearance of *Salmonella* infection in intestinal epithelial cells of mice [44]. Golovkine *et al.*, reported that ATG5, ATG7, and ATG16L1-mediated autophagy played a critical role in mice against *Mycobacterium tuberculosis* [45]. In the present study, we observed a marked increase in the expression of p-mTOR (at Ser 2448), with the elevated expression of LC3II protein and downregulated expression of Beclin1 in muscle tissues of infected mice, reflecting an inhibition of autophagy (Fig. 6). OST supplementation significantly inhibited the expression of p-mTOR and concomitantly upregulated the expression of LC3II and Beclin1 protein levels in the muscle tissue of infected mice, suggesting OST potentially activates autophagic clearance of *C. perfringens* (Fig. 6).

In conclusion, here we show for the first time OST supplementation provides protective effects against *C. perfringens* induced muscle myonecrosis in mice via the dual inhibition of oxidative stress and immuno-inflammatory response via the inhibition of p38, Erk1/2, NF- κ B pathways, and the activation of Nrf2/HO-1 and autophagy pathways. Our current data highlights the therapeutic potential of OST for the treatment of *C. perfringens* infection associated muscle pathogenesis in humans and animals.

Materials and methods

Chemicals and reagents

OST (purity >98%) was purchased from Chengdu Herb Purify Co., LTD (Chengdu, China). Aprotinin, leupeptin, pepstatin A, sodium dodecyl sulfonate (SDS), sulfinylbismethane (DMSO), and phenylmethylsulfonyl fluoride (PMSF) were purchased from Sigma-Aldrich (New York, NY, USA). RIPA Lysis Buffer, caspases-3, and -9 kits were purchased from Beyotime (Haimen, China). All other chemicals were the highest grade commercially available.

Bacteria culture

C. perfringens type A bacterial strain (C57-1) used in this study was purchased from the Institute of Veterinary Drug Control (Beijing, China). This strain was grown on brain heart infusion (BHI) broth at 37 °C in an anaerobic chamber (10% [vol/vol] H₂, 10% [vol/vol] CO₂, and 80% [vol/vol] N₂) (Oxoid Limited, UK). When an optical density at 600 (i.e., OD 600) was reached at about 0.5, the culture was centrifuged (8000 rpm, 10 min) and washed

two times with PBS, then, the number of colony-forming units (CFU) per 100 μ L was counted by plating serial 10-fold dilutions on BHI agar plates supplemented with yolk.

Animals and treatments

In this study, all animal experiments have been approved by the Institutional Animal Care and Use Committee at the China Agricultural University (No. CAU20230301-1). Male ICR mice (25–28 g, 8-week-old) were obtained from Beijing Vital River Animal Technology Co., Ltd. (Beijing, China). Mice had a 1-week acclimatization period before treatments. All mice had free access to food and water during experimental periods. All animal experiments were conducted in the isolation device of the experimental animal platform at China Agricultural University.

Mice were randomly divided into control, model, OST50, and OST100 treatment groups and 10 mice were in each group. Mice were intramuscularly injected once per day for 6 days at the femoral muscle site with 100 μ L PBS containing 1×10^8 CFU of *C. perfringens* C57-1 stain. In the OST50 and QST100 treatment groups, mice were firstly intramuscularly injected with 1×10^8 CFU of *C. perfringens* C57-1; after 1 h, mice were then injected intraperitoneally with OST at the doses of 50 and 100 mg/kg per day, respectively, and the treatments were continuous for 7 days. Mice in the untreated control group were treated with equal volume of vehicle (i.e., 0.5% DMSO). The detail experimental design was shown in Suppl. Figure 1. After 12 h of the last dose, mice were euthanized by sodium pentobarbital (80 mg/kg, intraperitoneal injection) and *C. perfringens*-infected femoral muscles were isolated for histopathological evaluations, and gene and protein expressions described below.

Histopathological examination of muscle tissues

After treatment, the *C. perfringens*-infected femoral muscles were isolated. Four samples were obtained in each group. Histopathological examinations were performed according to our published methods [46]. In brief, the isolated femoral muscle tissues were fixed in 4% paraformaldehyde and embedded in paraffin, and Hematoxylin–Eosin (H&E) staining was performed for light microscopic observation.

Gram staining for bacteria detection

Gram staining was performed using a Gram Stain Kit (Beijing Biorigin Science & Technology, Beijing, China) according to the provided protocol by the manufacturer. Briefly, the obtained sections were treated with a series of steps for removing paraffin and alcohol. Then, slices were

stained with the crystal violet dye on the sections to stain for 10 s–30 s. After washing, slices were stained with 1% iodine solution for 1 min and then were washed using water. Finally, slices were followed to tarnish using 95% ethanol (for 30 s) and re-stain using Double red dye (for 1 min). After staining, slices were observed in an optical microscope.

Measurement of malondialdehyde (MDA) levels, and superoxide dismutase (SOD) and catalase (CAT) activities in the muscle tissues of mice

The biomarkers of oxidative stress, including malondialdehyde (MDA) levels, superoxide dismutase (SOD), and catalase (CAT) activities in the muscle tissues of mice were examined via the commercially available MDA, SOD, and CAT reagent kits (Nanjing Jiancheng, Jiangsu, China). The protocols are strictly followed to the instructions of the reagent kits. Protein concentration of each sample was measured via a BCATM protein assay kit (Beyotime, Haimen, China). Finally, the values of MDA levels, and SOD, CAT activities were normalized to the protein concentration of each sample.

Measurement of caspases-3 and -9 activities in the muscle tissues of mice

The activities of caspases-3 and -9 in muscle tissues were measured, according to our previous study [32]. The protocols are strictly followed to the instructions of the reagent kits. Protein concentration of each sample was measured via a BCATM protein assay kit (Beyotime, Haimen, China). Finally, the values of caspases-3 and -9 activities were normalized to the protein concentration of each sample.

Measurement of protein expression in the muscle tissues of mice

The expression of protein markers involved MAPK, NF- κ B, and autophagy pathways in the muscle tissues of mice were examined using western blotting method, according to our previous description [47, 48]. About 10–20 mg tissues were added in the 1.5 mL-Eppendorf tube containing 0.5 mL RIPA buffer with multiple protease inhibitors (i.e., 1 mM PMSE, 1 μ g/mL aprotinin, 1 μ g/mL leupeptin, and 1 μ g/mL pepstatin A). After 10 min's incubation at 4 $^{\circ}$ C, the samples homogenized using a high-throughput protein homogenizer at 4 $^{\circ}$ C. After homogenization, the lysates were collected by centrifugation at 14,000 \times g for 15 min at 4 $^{\circ}$ C and the supernatants were collected. A BCA protein assay kit was used to measure the protein concentration of each sample. The gradient SDS-PAGE 8–15% gels were used to electrophoretic separation and a total of 30 μ g of protein were loaded in each lane. The primary antibodies, including polyclonal rabbit anti- microtubule-associated protein-1 light chain-3 (LC3), Nrf2, HO-1 (all 1:1000

dilution; ProteinTech Group, Chicago, IL, USA), Beclin1, NF- κ B (1:1000, Santa Cruz Biotechnology, TX, USA), phosphorylation (p)-mTORC1 (Ser 2448) p-p38, p-c-Jun N-terminal kinase 1/2 (JNK1/2), and p-Erk1/2 proteins (1:1000 dilution, Cell Signaling Technology, MA, USA), and mouse anti-glyceraldehyde-3-phosphate dehydrogenase (GAPDH) (1:10,000 dilution, Santa Cruz Biotechnology, TX, USA), were used in this study. The densitometric values of gel were quantified using ImageJ software (National Institute of Mental Health, Bethesda, MD, USA) and the relative expressed levels of all targeted protein were normalized to GAPDH protein.

Measurement of gene expression in the muscle tissues of mice

Muscle tissues of mice were collected and total RNA were extracted using the commercial total RNA Isolation Kit (No. RC112-01, Vazyme Biotech Co., Ltd., Nanjing, China), according to our previous study [49]. The quality of isolated RNA was assessed using a Nanodrop reader (Thermo Fisher Scientific, Shanghai, China). Then, a total of 1 μ g RNA was used to synthesize the cDNA by a Prime Script RT-PCR kit (Takara, Dalian, China). The PCR primers of all genes (including IL-1 β , Nrf2, HO-1, NF- κ B, TNF- α , and GAPDH) were provided in Suppl. Table 1. The qRT-PCR was performed by using the AB7500 real-time PCR instrument (Applied Biosystems, Foster City, CA, USA). The $2^{-\Delta\Delta C_t}$ method was used to calculate the relative transcript abundance of these targeted genes. GAPDH was set up as an endogenous control gene.

Statistical analysis

All results in the present study were presented as the mean \pm standard deviation (S.D.), unless otherwise specified. Comparisons among groups were performed using one-way analysis of variance, with post hoc correction by Tukey's method from the GraphPad Prism 9.0 software (GraphPad Software, Inc., La Jolla, CA, USA). A *P* value less than 0.05 was considered statistically significant.

Supplementary Information

The online version contains supplementary material available at <https://doi.org/10.1186/s44280-023-00028-6>.

Additional file 1: Suppl. Table 1. Primer sequences of the quantitative real-time PCR. **Suppl. Figure 1.** The experimental design in this study. **OST, osthole. Suppl. Figure 2.** The expression of NF- κ B (A), TNF- α (B), IL-1 β (C), Nrf2 (D), and HO-1 (D) mRNAs in the muscle tissues of mice.

Authors' contributions

C.D. conceived and designed the experiments; Z.X. and L.Y. performed the experiments; Z.X., L.Y., Z.S., and S.W. analyzed the data; C.D. wrote the paper; Z.S., C.W., D.L., and D.L. reviewed the paper. All authors have read and agreed to the published version of the manuscript.

Funding

This study was funded by Laboratory of Lingnan Modern Agriculture Project (Award number NT2021006). This study was also supported by the National Natural Science Foundation of China (Award number 32102724) and Pinduoduo-China Agricultural University Research Fund (No.PC2023A01002).

Availability of data and materials

Data will be shared upon request by the readers.

Declarations

Ethics approval and consent to participate

In this study, all animal experiments have been approved by the Institutional Animal Care and Use Committee at the China Agricultural University (No. CAU20230301-1).

Competing interests

The authors declare no conflict of interest.

Received: 3 August 2023 Revised: 8 October 2023 Accepted: 23 October 2023

Published online: 06 December 2023

References

- Low LY, Harrison PF, Gould J, Powell DR, Choo JM, Forster SC, et al. Concurrent host-pathogen transcriptional responses in a clostridium perfringens murine myonecrosis infection. *mBio*. 2018;9(2):e00473-18.
- Jong EC. Food poisoning: toxic syndromes. In: Jong EC, Sanford C, editors. *The travel and tropical medicine manual*. 4th ed. Edinburgh: WB. Saunders; 2008. p. 467–73.
- Monturiol-Gross L, Flores-Díaz M, Araya-Castillo C, Pineda-Padilla MJ, Clark GC, Titball RW, et al. Reactive oxygen species and the MEK/ERK pathway are involved in the toxicity of *Clostridium perfringens* α -toxin, a prototype bacterial phospholipase C. *J Infect Dis*. 2012;206(8):1218–26.
- Jing W, Pilato JL, Kay C, Feng S, Tuipulotu DE, Mathur A, et al. *Clostridium septicum* α -toxin activates the NLRP3 inflammasome by engaging GPI-anchored proteins. *Sci Immunol*. 2022;7(71):eabm1803.
- Park M, Rooney AP, Hecht DW, Li J, McClane BA, Nayak R, et al. Phenotypic and genotypic characterization of tetracycline and minocycline resistance in *Clostridium perfringens*. *Arch Microbiol*. 2010;192(10):803–10.
- Zong L, Teng D, Wang X, Mao R, Yang N, Hao Y, et al. Mechanism of action of a novel recombinant peptide, MP1102, against *Clostridium perfringens* type C. *Appl Microbiol Biotechnol*. 2016;100(11):5045–57.
- Goossens E, Valgaeren BR, Pardon B, Haesebrouck F, Ducatelle R, Deprez PR, et al. Rethinking the role of alpha toxin in *Clostridium perfringens*-associated enteric diseases: a review on bovine necro-haemorrhagic enteritis. *Vet Res*. 2017;48(1):9.
- Sakurai J, Nagahama M, Oda M. *Clostridium perfringens* alpha-toxin: characterization and mode of action. *J Biochem*. 2004;136(5):569–74.
- Takehara M, Seike S, Sonobe Y, Bandou H, Yokoyama S, Takagishi T, et al. *Clostridium perfringens* α -toxin impairs granulocyte colony-stimulating factor receptor-mediated granulocyte production while triggering septic shock. *Commun Biol*. 2019;2:45.
- Guo S, Li C, Liu D, Guo Y. Inflammatory responses to a *Clostridium perfringens* type A strain and α -toxin in primary intestinal epithelial cells of chicken embryos. *Avian Pathol*. 2015;44(2):81–91.
- Liu Y, Lei YX, Li JW, Ma YZ, Wang XY, Meng FH, et al. G protein-coupled receptor 120 mediates host defense against *Clostridium perfringens* infection through regulating NOD-like receptor family pyrin domain-containing 3 inflammasome activation. *J Agric Food Chem*. 2023;71(18):7119–30.
- Wang G, Liu H, Gao Y, Niu X, Deng X, Wang J, et al. Piceatannol alleviates *Clostridium perfringens* virulence by inhibiting perfringolysin O. *Molecules (Basel, Switzerland)*. 2022;27(16):5145.
- Zhang J, Liu S, Xia L, Wen Z, Hu N, Wang T, et al. Verbascoside protects mice from clostridial gas gangrene by inhibiting the activity of alpha toxin and perfringolysin O. *Front Microbiol*. 2020;11:1504.

14. Liu S, Yang X, Zhang H, Zhang J, Zhou Y, Wang T, et al. Amentoflavone attenuates *Clostridium perfringens* gas gangrene by targeting alpha-toxin and perfringolysin O. *Front Pharmacol*. 2020;11:179.
15. Liu S, Liu B, Luo ZQ, Qiu J, Zhou X, Li G, et al. The combination of osthole with baicalin protects mice from *Staphylococcus aureus* pneumonia. *World J Microbiol Biotechnol*. 2017;33(1):11.
16. Kordulewska NK, Topa J, Rozmus D, Jarmolowska B. Effects of osthole on inflammatory gene expression and cytokine secretion in histamine-induced inflammation in the caco-2 cell line. *Int J Mol Sci*. 2021;22(24):13634.
17. Li Z, Ji H, Song X, Hu J, Han N, Chen N. Osthole attenuates the development of carrageenan-induced lung inflammation in rats. *Int Immunopharmacol*. 2014;20(1):33–6.
18. Jin Y, Qian J, Ju X, Bao X, Li L, Zheng S, et al. Osthole protects against acute lung injury by suppressing NF- κ B-dependent inflammation. *Mediators Inflamm*. 2018;2018:4934592.
19. Kong L, Yao Y, Xia Y, Liang X, Ni Y, Yang J. Osthole alleviates inflammation by down-regulating NF- κ B signaling pathway in traumatic brain injury. *Immunopharmacol Immunotoxicol*. 2019;41(2):349–60.
20. Yang SM, Chan YL, Hua KF, Chang JM, Chen HL, Tsai YJ, et al. Osthole improves an accelerated focal segmental glomerulosclerosis model in the early stage by activating the Nrf2 antioxidant pathway and subsequently inhibiting NF- κ B-mediated COX-2 expression and apoptosis. *Free Radical Biol Med*. 2014;73:260–9.
21. Bao Y, Meng X, Liu F, Wang F, Yang J, Wang H, et al. Protective effects of osthole against inflammation induced by lipopolysaccharide in BV2 cells. *Mol Med Rep*. 2018;17(3):4561–6.
22. Huang W, Huang Y, Cui J, Wu Y, Zhu F, Huang J, et al. Design and synthesis of Osthole-based compounds as potential Nrf2 agonists. *Bioorg Med Chem Lett*. 2022;61:128547.
23. Kiu R, Hall LJ. An update on the human and animal enteric pathogen *Clostridium perfringens*. *Emerg Microbes Infect*. 2018;7(1):141.
24. Woittiez NJC, van Prehn J, van Immerseel F, Goossens E, Bauer MP, Rampeck CL, et al. Toxinotype A *Clostridium perfringens* causing septicaemia with intravascular haemolysis: two cases and review of the literature. *Int J Infect Dis*. 2022;115:224–8.
25. Awad MM, Bryant AE, Stevens DL, Rood JI. Virulence studies on chromosomal alpha-toxin and theta-toxin mutants constructed by allelic exchange provide genetic evidence for the essential role of alpha-toxin in *Clostridium perfringens*-mediated gas gangrene. *Mol Microbiol*. 1995;15(2):191–202.
26. Stevens DL, Titball RW, Jepson M, Bayer CR, Hayes-Schroer SM, Bryant AE. Immunization with the C-Domain of alpha -Toxin prevents lethal infection, localizes tissue injury, and promotes host response to challenge with *Clostridium perfringens*. *J Infect Dis*. 2004;190(4):767–73.
27. Zhou WB, Zhang XX, Cai Y, Sun W, Li H. Osthole prevents tamoxifen-induced liver injury in mice. *Acta Pharmacol Sin*. 2019;40(5):608–19.
28. Nagahama M, Michiue K, Sakurai J. Membrane-damaging action of *Clostridium perfringens* alpha-toxin on phospholipid liposomes. *Biochim Biophys Acta*. 1996;1280(1):120–6.
29. Grossman IW, Heitkamp DH, Sacktor B. Morphologic and biochemical effects of *Clostridium perfringens* alpha toxin on intact and isolated skeletal muscle mitochondria. *Am J Pathol*. 1967;50(1):77–88.
30. Manni MM, Valero JG, Pérez-Cormenzana M, Cano A, Alonso C, Goñi FM. Lipidomic profile of GM95 cell death induced by *Clostridium perfringens* alpha-toxin. *Chem Phys Lipid*. 2017;203:54–70.
31. Xia Y, Kong L, Yao Y, Jiao Y, Song J, Tao Z, et al. Osthole confers neuroprotection against cortical stab wound injury and attenuates secondary brain injury. *J Neuroinflammation*. 2015;12:155.
32. Dai C, Zhang X, Lin J, Shen J. Nootkatone supplementation ameliorates carbon tetrachloride-induced acute liver injury via the inhibition of oxidative stress, NF- κ B pathways, and the activation of Nrf2/HO-1 pathway. *Antioxidants (Basel)*. 2023;12(1):194.
33. Green DR, Reed JC. Mitochondria and apoptosis. *Science (New York, NY)*. 1998;281(5381):1309–12.
34. Liu Y, Liang J, Li JW, Xing LH, Li FX, Wang N, et al. Phagocyte extracellular traps formation contributes to host defense against *Clostridium perfringens* infection. *Cytokine*. 2023;169:156276.
35. Liu Y, Xing LH, Li FX, Wang N, Ma YZ, Li JW, et al. Mixed lineage kinase-like protein protects against *Clostridium perfringens* infection by enhancing NLRP3 inflammasome-extracellular traps axis. *iScience*. 2022;25(10):105121.
36. Liao PC, Chien SC, Ho CL, Wang EI, Lee SC, Kuo YH, et al. Osthole regulates inflammatory mediator expression through modulating NF- κ B, mitogen-activated protein kinases, protein kinase C, and reactive oxygen species. *J Agric Food Chem*. 2010;58(19):10445–51.
37. Fan H, Gao Z, Ji K, Li X, Wu J, Liu Y, et al. The *in vitro* and *in vivo* anti-inflammatory effect of osthole, the major natural coumarin from *Cnidium monnieri* (L.) Cuss, via the blocking of the activation of the NF- κ B and MAPK/p38 pathways. *Phytomedicine*. 2019;58:152864.
38. Oda M, Shiihara R, Ohmae Y, Kabura M, Takagishi T, Kobayashi K, et al. *Clostridium perfringens* alpha-toxin induces the release of IL-8 through a dual pathway via TrkA in A549 cells. *Biochim Biophys Acta*. 2012;1822(10):1581–9.
39. Monturiol-Gross L, Flores-Díaz M, Pineda-Padilla MJ, Castro-Castro AC, Alape-Giron A. *Clostridium perfringens* phospholipase C induced ROS production and cytotoxicity require PKC, MEK1 and NF κ B activation. *PLoS One*. 2014;9(1):e86475.
40. Tang H, Li K, Dou X, Zhao Y, Huang C, Shu F. The neuroprotective effect of osthole against chronic sleep deprivation (CSD)-induced memory impairment in rats. *Life Sci*. 2020;263:118524.
41. García-Arroyo FE, Gonzaga-Sánchez G, Tapia E, Muñoz-Jiménez I, Manteola-Romero L, Osorio-Alonso H, et al. Osthol ameliorates kidney damage and metabolic syndrome induced by a high-fat/high-sugar diet. *Int J Mol Sci*. 2021;22(5):2431.
42. Itakura E, Mizushima N. Characterization of autophagosome formation site by a hierarchical analysis of mammalian Atg proteins. *Autophagy*. 2010;6(6):764–76.
43. Dai C, Xiao X, Li D, Tun S, Wang Y, Velkov T, et al. Chloroquine ameliorates carbon tetrachloride-induced acute liver injury in mice via the concomitant inhibition of inflammation and induction of apoptosis. *Cell Death Dis*. 2018;9(12):1164.
44. Conway KL, Kuballa P, Song JH, Patel KK, Castoreno AB, Yilmaz OH, et al. Atg1611 is required for autophagy in intestinal epithelial cells and protection of mice from *Salmonella* infection. *Gastroenterology*. 2013;145(6):1347–57.
45. Golovkine GR, Roberts AW, Morrison HM, Rivera-Lugo R, McCall RM, Nilsson H, et al. Autophagy restricts mycobacterium tuberculosis during acute infection in mice. *Nat Microbiol*. 2023;8(5):819–32.
46. Takehara M, Kobayashi K, Nagahama M. Toll-like receptor 4 protects against *Clostridium perfringens* infection in mice. *Front Cell Infect Microbiol*. 2021;11:633440.
47. Dai C, Li M, Sun T, Zhang Y, Wang Y, Shen Z, et al. Colistin-induced pulmonary toxicity involves the activation of NOX4/TGF- β /mtROS pathway and the inhibition of Akt/mTOR pathway. *Food Chem Toxicol*. 2022;163:112966.
48. Dai C, Zhang Q, Shen L, Sharma G, Jiang H, Wang Z, et al. Quercetin attenuates quercetone-induced cell apoptosis *in vitro* by activating the P38/Nrf2/HO-1 Pathway and inhibiting the ROS/mitochondrial apoptotic pathway. *Antioxidants (Basel)*. 2022;11(8):1498.
49. Dai C, Liu M, Zhang Q, Das Gupta S, Tang S, Shen J. Nootkatone supplementation attenuates carbon tetrachloride exposure-induced nephrotoxicity in mice. *Antioxidants (Basel)*. 2023;12(2):370.

Publisher's Note

Springer Nature remains neutral with regard to jurisdictional claims in published maps and institutional affiliations.

Ready to submit your research? Choose BMC and benefit from:

- fast, convenient online submission
- thorough peer review by experienced researchers in your field
- rapid publication on acceptance
- support for research data, including large and complex data types
- gold Open Access which fosters wider collaboration and increased citations
- maximum visibility for your research: over 100M website views per year

At BMC, research is always in progress.

Learn more biomedcentral.com/submissions

